Instantaneous information propagation in free flow, synchronized flow, stop-and-go waves in a cellular automaton model

Rui Jiang[1], Wen-Long Jin[2], Qing-Song Wu[1]

[1]School of Engineering Science, University of Science and Technology of China, Hefei 230026, P.R.China

[2]Department of Automation, University of Science and Technology of China, Hefei 230026, P.R.China

Abstract: Recently, a number of efforts are underway to investigate inter-vehicle communications (IVC). In this paper, we have studied the instantaneous information propagation behaviors based on IVC in three different traffic situations (free flow, synchronized flow and stop-and-go waves) in a cellular automaton model. It is shown that different behaviors appear in stop-and-go waves from that in free flow and synchronized flow. While the distribution of Multi-hop Communication Distance (MhCD) is either exponential or uniform in free flow and synchronized flow, the distribution of MhCD is either exponential or with a single peak in stop-and-go waves.

1. Introduction

Intelligent transportation systems (ITS) that incorporate advanced technologies have been purported to offer efficiencies in tackling traffic congestion. The rapid advance in available information technology, especially, the development of wireless

communication technologies, now makes feasible the exploration of traffic information systems that decentralize the tasks of collecting and disseminating traffic information. A number of efforts are currently underway to investigate inter-vehicle communications (IVC) based on mobile ad hoc networking technology as a means of developing "internet on the road" (e.g., [1-3]).

This paper focuses on a fundamental issue regarding to performance of such a system; i.e., how far can information be expected to propagate in a traffic system under certain traffic conditions, penetration rate of equipped cars, and transmission range of wireless units? By providing some general answers to this question, we hope to help guide specification of appropriate communication devices, routing protocols, and database management schemes that would be required in order to have the most important information collected and distributed, and to determine the range of applications for which a mobile, ad hoc traffic information system might be effective.

In previous work, Hartenstein et al. [4] simulated the process of information propagation using the cellular automaton model, presenting results on the probability that two equipped vehicles could establish connection through IVC under different transmission ranges. In [5], IVC was simulated with Paramics, a microscopic traffic simulator, and the maximum information propagation distance was evaluated against transmission range and penetration rate for unidirectional roads, bi-directional roads, and road networks. In [6], propagation of travel time information was studied in a grid

road network through information exchange between vehicles traveling in opposite directions. Jin and Recker [7] developed an analytical model of the probability that a message can travel beyond a point in a traffic stream on a link.

The empirical observations show that in real traffic, there exist complex traffic phenomena such as synchronized flow, stop-and-go waves etc. As noted in [7], traffic patterns have significant influences on the distribution of the locations of equipped vehicles and therefore on the performance of IVC. However, in the previous studies, the information propagation behaviors were only studied for very simple scenarios of uniform or piecewisely uniform traffic streams, but not identified for stop-and-go waves or synchronized flow.

In this paper, the problem is investigated using a cellular automaton (CA) traffic flow model. Recently, modeling road traffic behavior using CA has become a well-established method to model, analyze, understand, and even forecast the behavior of real road traffic, because the automata's evolution rules are simple, straightforward to understand, computationally efficient and sufficient to emulate much of the behavior of observed traffic flow [8-19]. We study the dependence of Multi-hop Communication Distance (MhCD), i.e., the distance a piece of information propagates, on the transmission range R and the penetration rate of equipped vehicles μ in free flow, synchronized flow and in stop-and-go waves. As in [7], we assume that (i) the transmission range R is constant for each hop; (ii) the traffic stream is static, as

compared to the information propagation (i.e., instantaneous information propagation behaviors).

In the next Section, the CA model used in this paper is introduced. It is shown that free flow, synchronized flow and stop-and-go waves can be induced by speed limit bottleneck (of different limit speed v_{lim}). In Section 3, the instantaneous information propagation behaviors for various traffic patterns are investigated. The conclusions are given in Section 4.

2. Cellular automaton simulation

2.1 A CA Model

In this Section, the CA model used for simulation is introduced. In the CA models, the roads are classified into cells, a cell is either occupied by a vehicle or empty. The vehicles move with velocity 0, 1, 2, ..., v_{max}, where v_{max} is an integer representing the maximum velocity of the vehicles.

Recently, the authors have introduced a CA model, which can reproduce the empirical traffic situation quite satisfactorily [17-19]. In the model, the parallel update rules of the model are as follows:

• Determination of the randomization parameter p_n(t+1), which takes into account the different behavioral patterns of the individual drivers, especially, nondeterministic acceleration as well as overreaction while slowing down:

$p_n(t+1)=p(v_n(t), b_{n+1}(t), t_{h,n}, t_{s,n})$

• Acceleration:

if $((b_{n+1}(t)=0$ or $t_{h,n} \geq t_{s,n})$ and $v_n(t)>0))$ then $v_n(t+1)=$ **min**$(v_n(t)+2, v_{max})$

else if $(v_n(t)=0)$ then $v_n(t+1)=$ **min**$(v_n(t)+1, v_{max})$

else $v_n(t+1)=v_n(t)$

• Braking rule:

$v_n(t+1)=$**min**$(d_n^{eff}, v_n(t+1))$

• Randomization and braking:

if (rand()$<p_n(t+1)$) then: $v_n(t+1)=$ **max**$(v_n(t+1)-1, 0)$

• Determination of $b_n(t+1)$:

if $((v_n(t+1)>v_n(t))$ or $(v_n(t+1) \geq v_c$ and $t_{f,n}>t_{c1}))$ then: $b_n(t+1)=0$

else if $(v_n(t+1)<v_n(t))$ then: $b_n(t+1)=1$

else $(v_n(t+1)=v_n(t))$ then: $b_n(t+1)=b_n(t)$

• Determination of $t_{st,n}$

if $v_n(t+1)=0$ then: $t_{st,n}=t_{st,n}+1$

if $v_n(t+1)>0$ then: $t_{st,n}=0$

• Determination of $t_{f,n}$:

if $v_n(t+1) \geq v_c$ then: $t_{f,n}=t_{f,n}+1$

if $v_n(t+1) < v_c$ then: $t_{f,n}=0$

• Car motion:

$x_n(t+1)=x_n(t)+v_n(t+1)$.

Here $x_n(t)$ and $v_n(t)$ are the position and velocity of vehicle n at time instant t (here vehicle $n+1$ precedes vehicle n), d_n is the gap of the vehicle n, b_n is the status of the brake light (on(off)→ $b_n=1(0)$). The two times $t_{h,n} = d_n/v_n(t)$ and $t_{s,n}=\mathbf{min}(v_n(t)(\delta t)/(\delta v), h)$, where h determines the range of interaction with the brake light, are introduced to compare the time $t_{h,n}$ needed to reach the position of the leading vehicle with a velocity dependent interaction horizon $t_{s,n}$, $d_n^{eff} = d_n+\mathbf{max}(v_{anti}-gap_{safety},0)$ is the effective distance, where $v_{anti}=\mathbf{min}(d_{n+1},v_{n+1})$ is the expected velocity of the preceding vehicle in the next time step and gap_{safety} controls the effectiveness of the anticipation. rand() is a random number between 0 and 1, $t_{st,n}$ denotes the time that the car n stops, $t_{f,n}$ denotes the time that car n is in the state $v_n \geq v_c$. The randomization parameter p is defined:

$$p(v_n(t), b_{n+1}(t), t_{h,n}, t_{s,n}) = \begin{cases} p_b: \text{ if } b_{n+1} = 1 \text{ and } t_{h,n} < t_{s,n} \\ p_o: \text{ if } v_n = 0 \text{ and } t_{st,n} \geq t_c \\ p_d: \text{ in all other cases} \end{cases}$$

Here $\delta t=1$, $\delta v=1$, $t_c=7$, $t_{c1}=30$ and $v_c=18$ are parameters.

2.2 Simulation Set-up

In the simulations, the open boundary conditions are used. In one time step, when the update of the cars on the road is completed, we check the position (the first cell) of the last car and that of the leading car on the road, which are denoted as x_{last} and x_{lead}, respectively. If $x_{last} > v_{\max}$, a car with velocity $v_{\max}$ is injected with probability α at the

cell **min**(x_{last} $-v_{\max}$, $v_{\max}$). Near the exit of the road, the leading car is removed if $x_{lead}>L$ (L denotes the position of the right most cell on road) and the following car becomes the new leading car and it moves without any hindrance. The length of the test single-lane road is L=30000 cells. Initially there is no car on the road. From t=0 on, the cars drive into the road with probability α. We assume there is a speed limit region from x=24900 to x=25000 cells, in which the maximum velocity of vehicles is $v_{\lim}$.

In the simulations, the parameter values are $v_{\max}$=20 (corresponding to 108 km/h), p_d=0.1, p_b=0.94, p_0=0.5, h=6, gap_{safety}=7. Each cell corresponds to 1.5 m and a vehicle has a length of five cells. One time step corresponds to 1 s.

2.3 Three Phases of Traffic Flow

Recently, based on his empirical observations, Kerner developed a three phase traffic theory [13]. In the theory, traffic can be either free or congested, and congested flow is further classified into synchronized flow and jams. While the jams are characterized by constant mean velocity of the downstream jam front, the downstream front of synchronized flow is often fixed at a bottleneck. Moreover, the onset of congestion is usually associated with a phase transition from free flow to synchronized flow and jams can merge spontaneously in synchronized flow.

In Fig.1, we show typical free flow, synchronized flow, and stop-and-go waves

induced by the speed limit bottleneck of different v_{lim}. In all three figures, we have a free flow region downstream to the bottleneck. In Figure 1a, since the capacity of the speed limit region is higher than the demand level at the entrance, free flow with density and speed at 15.5 vehicles/km and 107 km/h respectively is maintained upstream to the bottleneck. In Figure 1b, the capacity of the speed limit region is lower than the demand level at the entrance; as a result, the congestion, i.e., synchronized flow with density and speed at 33.9 vehicles/km and 50 km/h respectively, appears. When v_{lim} is very small, the stop-and-go waves occur (Figure 1c). But note that, near the speed limit region, synchronized flow exists. In the nextsection, we investigate the instantaneous information propagation behaviors in the three different kinds of traffic situations, respectively.

3. Instantaneous information propagation behaviors

3.1 Free Flow

Firstly, we investigate instantaneous information propagation behaviors in free flow shown in (Figure 1a). We focus on the Multi-hop Communication Distance (MhCD), i.e., the distance a piece of information propagates, of the first equipped vehicles upstream of the speed limit region. Here we only consider information propagation in the opposite direction of traffic flow. Figure 2 shows the probability distribution of MhCD at various distances in the free flow for different market penetration rate. The probability distribution is obtained from 150000 samples and each data point on the

curve denotes the probability that MhCD is in the range $200M \le MhCD < 200(M+1)$, with M=0,1,2,…One can see that the curve is nearly a straight line (with some fluctuations) in the semi-log plane, which means the MhCD obeys an exponential distribution. With the increase of penetration rate μ, the slope (absolute value) decreases.

Figure 3 shows the probability distribution of MhCD in the free flow where the transmission range R is larger (R=200 cells). One can see that for μ=0.2, 0.4, and 0.6, the exponential distribution of MhCD exists as in Figure 2. However, when μ=0.8 and 1, the information could propagate to the entrance of the road section, i.e., the maximum MhCD is larger than the length of the study area. Therefore, the peak of the distribution curve at MhCD≈25000 means the probability that the information could propagate to the entrance of the road section.

Figure 4 shows the distribution of MhCD in the free flow where the transmission range R=400. One can see that when μ=0.8 and 1, the distribution of MhCD is nearly uniform for $MhCD<MhCD_m\approx24500$. Note that the uniform distribution of MhCD means the success rate of information propagation is linearly decreasing with the information propagation distance. With the increase of μ, the appearance probability of MhCD smaller than $MhCD_m$ decreases.

Figure 5 shows the distribution of MhCD in the free flow in a larger system where

L=60000. The speed limit region is from x=54900 to x=55000. Comparing Figure 5 with Figure 4, one can see that the distributions are the same for MhCD<$MhCD_c$ as shown by the dashed line. Based on this, we argue that in an infinite system, the distribution of MhCD is either exponential or uniform (for not so large R and/or μ). When R and/or μ are large enough, the uniform probability becomes zero and the information can propagate to infinity.

3.2 Synchronized Flow

We investigate the instantaneous information propagation behaviors in synchronized flow (Figure 1b). Figure 6 shows the distribution of MhCD in the synchronized flow. One can see that similar to that in free flow, the distribution of MhCD is exponential when penetration rate μ is not so large (Figure 6a). For very large μ, the distribution becomes uniform (Figure 6b). With the increase of R, the transition from exponential distribution to uniform distribution occurs at a smaller penetration rate μ.

In Figure 7, we compare the average MhCD and the variance of MhCD in free flow and in synchronized flow. One can see that both are larger in synchronized flow. This is because the density is larger in synchronized flow. Therefore, the average distance between two consecutive vehicles is smaller, which is better for the information to propagate.

3.3 Stop-and-Go Waves

Finally we investigate the instantaneous information propagation behaviors in stop-and-go waves (Figure 1c). Figure 8 shows the distribution of MhCD in the stop-and-go waves. When the transmission range R and the penetration rate μ are small, the information cannot propagate far. Since near the speed limit region, the synchronized flow exists, the distribution of MhCD is exponential (μ=0.2 and 0.3, Figure 8a). When μ increases, the information can propagate into the stop-and-go region. As a result, the distribution of MhCD is not exponential (μ=0.4, Figure 8a): a peak begins to appear (μ=0.6, Figure 8). If μ continues increasing, the distribution expands and the peak decreases and shifts right. When μ=1, the information could propagate to the entrance of the road section, accordingly another peak of the distribution curve appears at MhCD≈25000.

Figure 9 shows the distribution of MhCD in the stop-and-go waves where the transmission range R is larger. Similar results are obtained. Based on this, we argue that in an infinite system, the distribution of MhCD is with a single peak when R and/or μ are large.

4. Conclusion

IVC is widely regarded as a promising concept for the transmission of traffic-related

information. In contrast to classical communication channels, which operate with a centralized broadcast concept via radio or mobile-phone services, IVC is designed as a local service without central station and without the need for additional infrastructure. Apart from the drivers appreciating reliable and up-to-date traffic information, the whole traffic system may benefit from IVC as well.

This paper focuses on how far information can be expected to propagate in a traffic system under different traffic conditions. To this end, a CA model which can describe free flow, synchronized flow and stop-and-go waves is used.

Our simulations show that different behaviors appear in stop-and-go waves from that in free flow and synchronized flow. In free flow and synchronized flow, the distribution of MhCD is exponential when the transmission range R and penetration rate μ are small. However, with the increase of R and/or μ, the slope of the distribution (absolute value) decreases. When R and/or μ are large enough, the distribution becomes uniform. The uniform probability decreases with the further increase of R and/or μ.

In stop-and-go waves, the distribution of MhCD is still exponential when the transmission range R and penetration rate μ are small. However, with the increase of R and/or μ, the distribution transits into one with a single peak. Then the distribution expands and the peak decreases and shifts right with the further increase of R and/or

μ.

In our future work, the investigation will be extended to bi-directional traffic and to network (which is a dynamically changing ad hoc network). We will consider that the network dynamics strongly influences message propagation, which is done by the movement of nodes (vehicles) and by hops between nearby nodes.

Acknowledgements

We acknowledge the support of National Basic Research Program of China (2006CB705500), the National Natural Science Foundation of China (NNSFC) under Key Project no. 10532060 and Project nos. 10404025, 10672160, 70601026, and the CAS special Foundation.

References

1. CarTALK 2000. Safe and comfortable driving based upon inter-vehicle communication. http://www.cartalk2000.net/.
2. FleetNet. Internet on the road. http://www.fleetnet.de/
3. M. Schoenhof, A. Kesting, M. Treiber, D. Helbing, Coupled vehicle and information flows: Message transport on a dynamic vehicle network. Physica A, Vol. 363, 73-81 (2006); M. Schoenhof, A. Kesting, M. Treiber, D. Helbing, Inter-vehicle communication on freeways: statistical properties of information propagation in ad-hoc networks. Traffic and Granular flow 05' (to appear).
4. H. Hartenstein, B. Bochow, A. Ebner, et al., Position-aware ad hoc wireless

networks for inter-vehicle communications: the fleetnet project. In: Proceedings of the 2nd ACM International Symposium on Mobile ad hoc Networking and Computing, Long Beach, CA, USA, 2001, 259–262.

5. X.Yang, Assessment of a self-organizing distributed traffic information system: modeling and simulation. Ph.D. thesis, University of California, Irvine, 2003.
6. A.K. Ziliaskopoulos, J. Zhang, A zero public infrastructure vehicle based traffic information system. In: Transportation Research Board 2003 Annual Meeting CD-ROM, Washington, DC, 2003.
7. W.L.Jin, W.W.Recker, Instantaneous information propagation in a traffic stream through inter-vehicle communication. Transpn.Res.B Vol.40, 230-250 (2006).
8. B.S.Kerner, S.L.Klenov and D.E.Wolf, Cellular automata approach to three phase traffic theory. J.Phys.A, **35**, 9971-10013 (2002).
9. D.Chowdhury, L.Santen, and A.Schadschneider, Statistical physics of vehicular traffic and some related systems. Phys.Rep. **329**, 199-329 (2000).
10. D.Helbing, Traffic and related self-driven many-particle systems. Rev.Mod.Phys. **73**, 1067-1114 (2001).
11. T.Nagatani, The physics of traffic jams. Rep.Prog.Phys. **65**, 1331-1386 (2002).
12. K. Nagel, P. Wagner, and R. Woesler. Still flowing: Approaches to traffic flow and traffic jam modeling. Operations Research, **51**(5), 681–710, 2003.
13. B.S. Kerner, *The Physics of Traffic* (Springer, Berlin, New York, 2004).
14. *Traffic and Granular Flow '03*, edited by S.P.Hoogendoorn, P.H.L.Bovy, M.Schreckenberg, and D.E.Wolf (Springer, Heidelberg, 2005)

15. M.E. Lárraga, J.A. del Río and L. Alvarez-lcaza, cellular automata for one-lane traffic flow modeling. Transpn.Res.C **13**, 63-74 (2005).
16. B.S.Kerner and S.L.Klenov, Microscopic theory of spatial-temporal congested traffic patterns at highway bottlenecks. Phys.Rev.E **68**, 036130 (2003).
17. R.Jiang and Q.S.Wu, Cellular automata models for synchronized traffic flow. J.Phys.A, **36**, 381-390 (2003).
18. R.Jiang and Q.S.Wu, Spatial–temporal patterns at an isolated on-ramp in a new cellular automata model based on three-phase traffic theory. J.Phys.A **37**, 8197-8213 (2004).
19. R.Jiang and Q.S.Wu, First order phase transition from free flow to synchronized flow. Euro.Phys.J.B (2005).

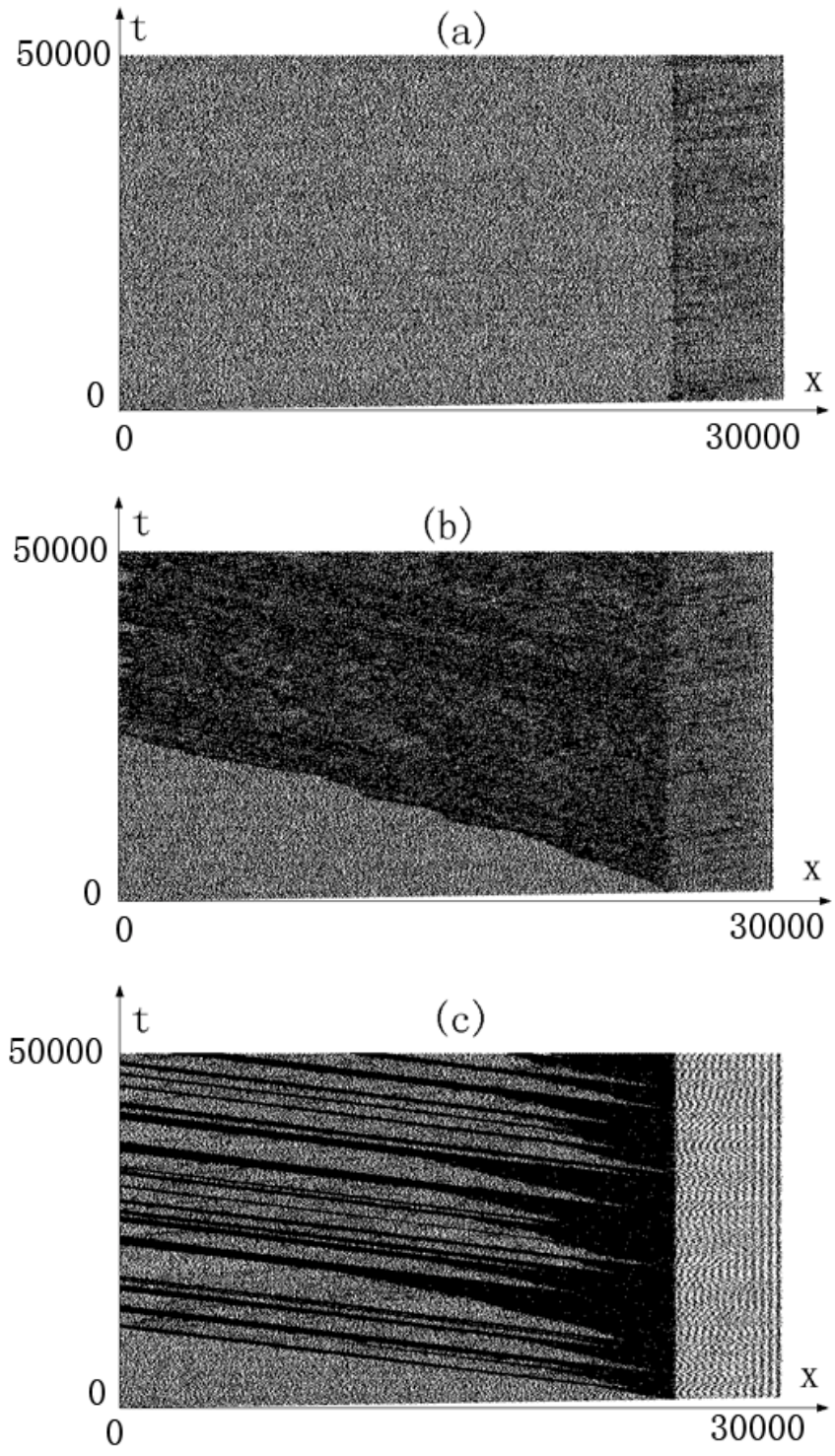

Figure 1: Typical free flow (a), synchronized flow (b), and stop-and-go waves (c) induced by the speed limit bottleneck. In (a) α=0.46, v_{lim}=15; (b) α=0.5, v_{lim}=15; (c) α=0.46, v_{lim}=4.

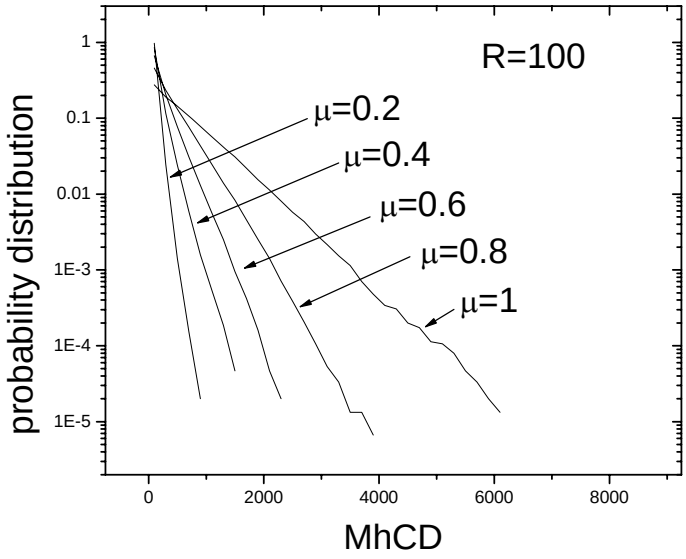

Figure 2: Probability distribution of MhCD in free flow. The transmission range R=100.

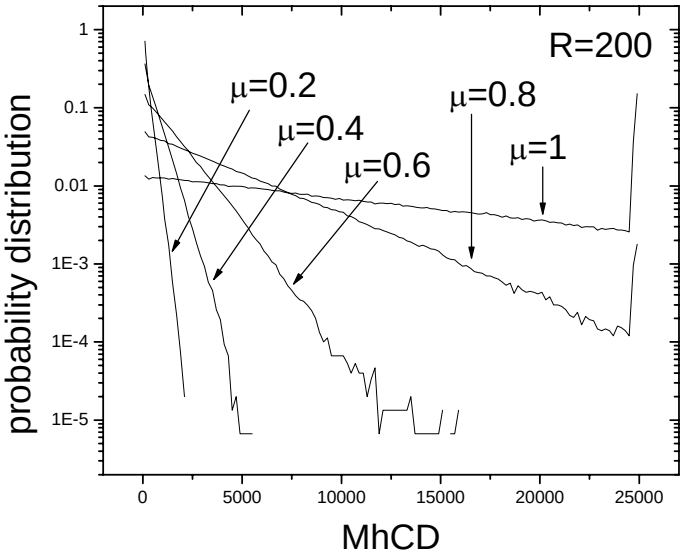

Figure 3: Probability distribution of MhCD in free flow. The transmission range R=200.

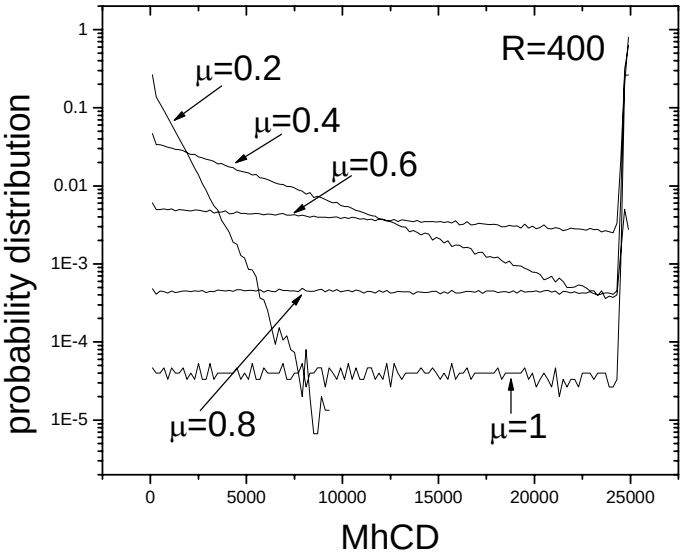

Figure 4: Probability distribution of MhCD in free flow. The transmission range R=400.

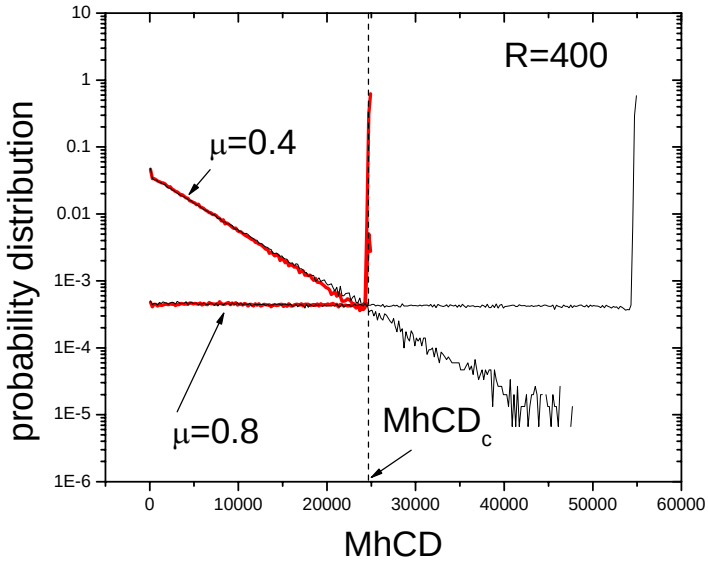

Figure 5: Probability distribution of MhCD in free flow in system of L=30000 (red lines) and L=60000 (black lines).

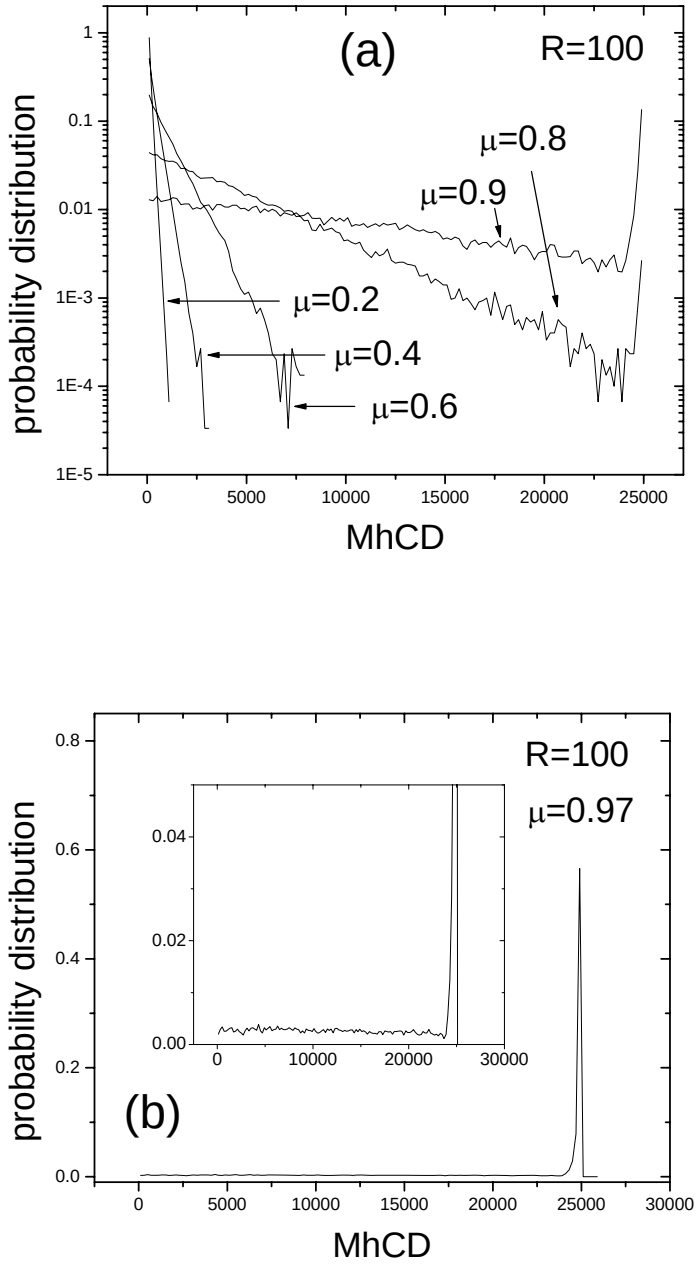

Figure 6: Probability distribution of MhCD in synchronized flow in system of L=30000. In (b), the inset shows the details of the uniform distribution.

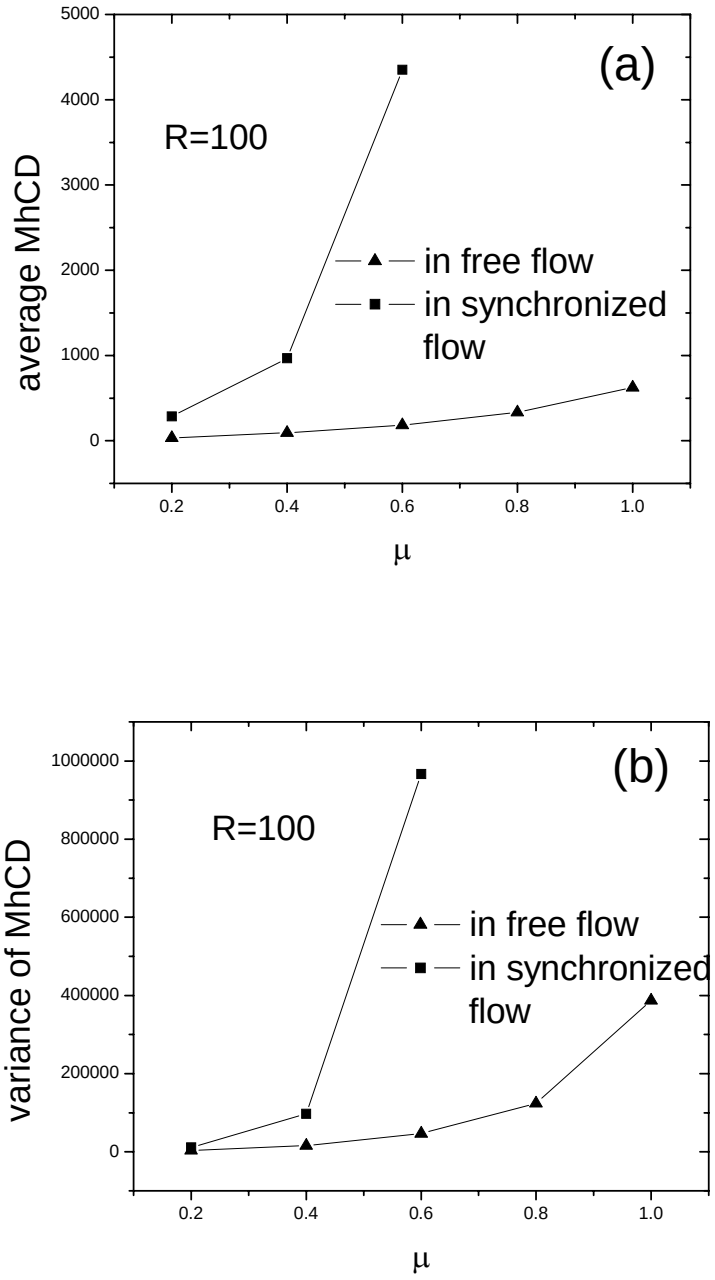

Figure 7: Comparison of average MhCD and variance of MhCD in free flow and synchronized flow.

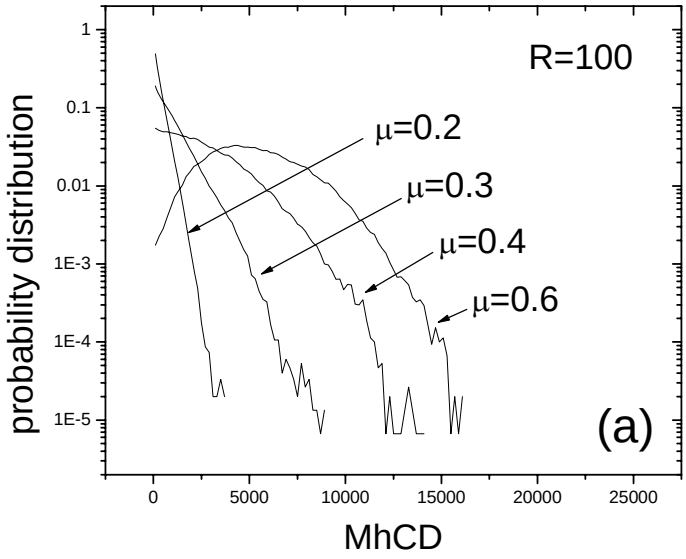

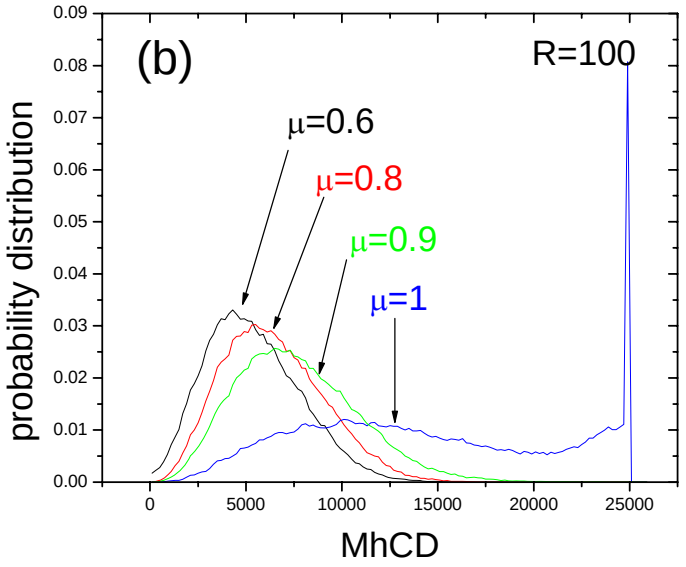

Figure 8: Probability distribution of MhCD in stop-and-go waves in system of L=30000. The transmission range R=100.

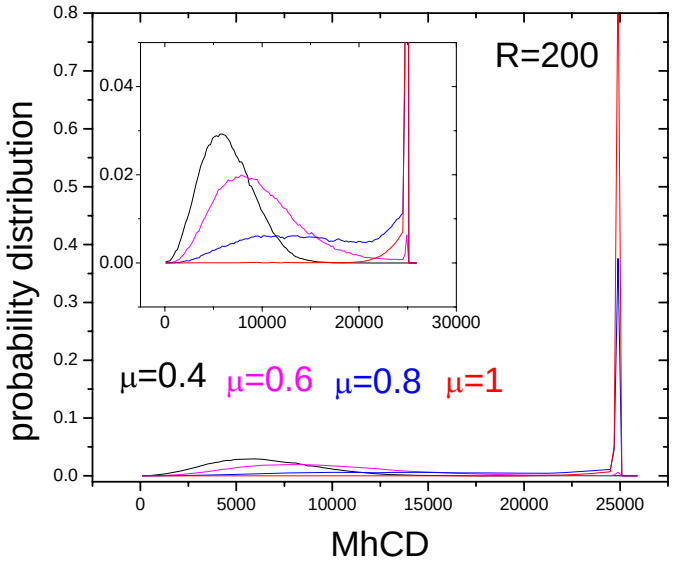

Figure 9: Probability distribution of MhCD in stop-and-go waves in system of L=30000. The transmission range R=200. The inset shows the details of the peak of the distribution.